



Conference Proceedings of the 4th Asia Pacific Luminescence and Electron Spin Resonance Dating Conference
Nov 23rd-25th, 2015, Adelaide, Australia

Guest Editor: Lee Arnold

COARSE VERSUS FINE-GRAIN QUARTZ OPTICAL DATING OF THE SEDIMENTS RELATED TO THE 1985 Ms7.1 WUQIA EARTHQUAKE, NORTHEASTERN MARGIN OF THE PAMIR SALIENT, CHINA

HUILI YANG¹, JIE CHEN¹, NAOMI PORAT², TAO LI³, WENQIAO LI⁴ and WEIPENG XIAO⁵

¹State Key Laboratory of Earthquake Dynamics, Institute of Geology, China Earthquake Administration, Beijing 100029, China

²Geological Survey of Israel, 30 Malkhe Israel Street, Jerusalem 95501, Israel

³Guangdong Provincial Key Lab of Geodynamics and Geohazards, School of Earth Sciences and Engineering, Sun Yat-sen University, Guangzhou 510275, China

⁴Institute of Earthquake Science, China Earthquake Administration, Beijing 100036, China

⁵Anhui Earthquake Administration, Hefei 230031, China

Received 31 January 2016

Accepted 19 May 2017

Abstract: Optical dating of earthquake related sediments were investigated including one modern sample and three samples from a trench excavated across the 1985 Ms7.4 Wuqia Earthquake surface rupture. The results indicated that equivalent dose (D_e) values vary with grain size and the method used for D_e determination. The residual dose of the modern sample is 0.1 ka ($0.2_{-0.1}^{+0.2}$ Gy) for the quartz single grain measurements. Only 1.5–3.6% of the grains have a detectable OSL signal. Single grain quartz ages are similar to the expected ages. Fine grain quartz results overestimate the D_e values and are much older than single grain quartz and coarse grain quartz small aliquot standardized growth curve (SA-SGC) ages. Single grain quartz OSL dating may be optimal for dating earthquake related deposits, but SA-SGC can save measurement time and has potential for dating some poorly bleaching samples.

Keywords: paleo-earthquake, quartz OSL dating, single grain, coarse grain.

1. INTRODUCTION

Dating paleo-earthquake events is very important for estimating earthquake hazards. High-resolution and high-precision dating of seismic events that help to calculations of recurrence intervals on timescales of decades to several thousand years is challenging, particularly in

semi-arid to arid settings, where organic debris for ^{14}C dating is uncommon. Recent studies (e.g., Banerjee *et al.*, 2001; Lu *et al.*, 2007; Porat *et al.*, 2009; Fattahi *et al.*, 2010; Liu *et al.*, 2010; Wang *et al.*, 2012) have shown that optical dating of earthquake-related deposits is capable of producing robust chronologies of paleo-earthquake events. However, a potential problem in such settings is that light exposure of earthquake-related sediments may have been insufficient to fully reset (bleach) the OSL signal prior to deposition (Cunha *et al.*, 2009; Yang *et al.*, 2012).

Corresponding author: J. Chen
e-mail: mailto:chenjie@ies.ac.cn

Incomplete resetting of the OSL signal will lead to age overestimation. Fuchs *et al.* (2005) and Olley *et al.* (1998) examined the dependence of bleaching on grain size. It is now well known that quartz OSL signals bleach more easily than feldspar IRSL (infrared stimulated luminescence) signals (Yang *et al.*, 2012), and in many cases it appears that coarse grain (74–250 μm) bleaches better than fine grain (4–11 μm) quartz (Yang *et al.*, 2012). But in fact, samples from different depositional environments may have different bleaching characteristic.

The August 23, 1985 Ms7.1 Wuqia Earthquake ruptured the eastern segment of the seismically active Pamir Front Thrust at the leading northeastern edge of the Pamir salient of the Tibetan Plateau, producing a 15-km long surface fault scarps, and destroying the old Wuqia town (Feng *et al.*, 1986). Data on the recurrence period of such devastating earthquakes is a vital input for seismic hazard evaluation and risk assessment in this region. In this study, we test one modern sample and three samples from a trench excavated across the 1985 Wuqia Earthquake surface rupture (Fig. 1) using a variety of techniques on fine grain quartz (FQ) and coarse grain quartz (CQ). The purpose is to test assumptions regarding the zeroing of the deposition after the Wuqia earthquake, to assess which grain sizes are most appropriate and which dating technique can provide reliable ages for earthquake related

rapidly-deposited sediments. Finally we also applied time-saving protocols such as small aliquot standardised growth curve (SA-SGC) (Roberts and Duller, 2004; Lai *et al.*, 2007, Li *et al.*, 2015) to check its potential for dating heterogeneously reset samples.

2. MATERIALS AND METHODS

Samples and instruments

A trench (Fig. 2b) was excavated across a small sag pond of the 1985 Ms7.1 Wuqia Earthquake surface fault scarp at a fluvial terrace and exposed a sequence of slope deposited silts and sands mainly sourced from the Pliocene sandstone and siltstone rocks 200 m to the north (Fig. 1). Four earthquake events including the 1985 event were identified in the trench. Three samples deposited before the 1985 earthquake were collected from trench, and one sample deposited after the 1985 earthquake (Fig. 2 Left) were selected as a known age sample. Cosmogenic ^{10}Be depth-profile ages on detrital sand and pebble from a trench on the same terrace several km to the west from our study area (Fig. 1 CRN sample) are 8.0 ± 1.1 ka and 8.8 ± 1.5 ka, respectively (Thompson, 2013). The OSL samples we collected are deposited on top of the same terrace surface, should be younger than 8.0 ka.

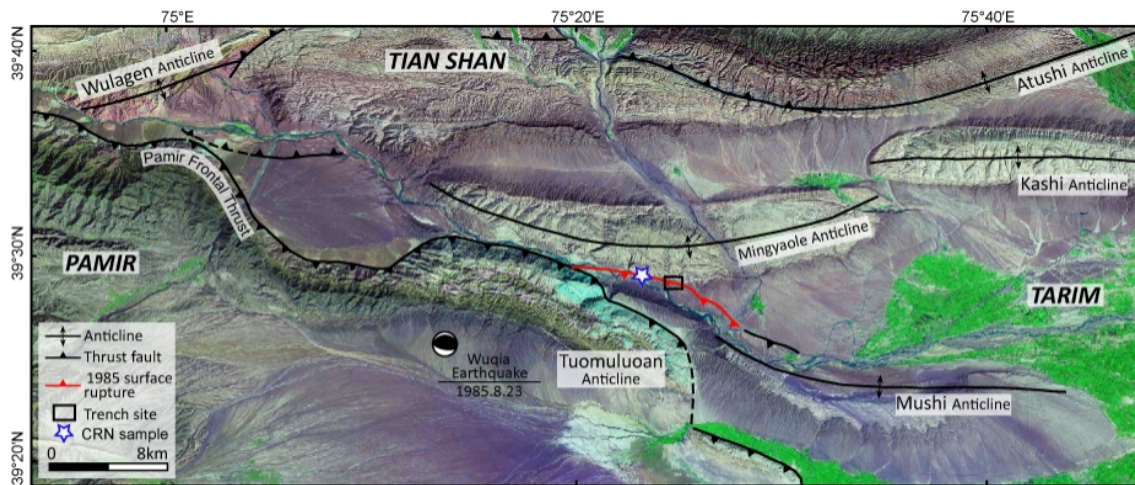


Fig. 1. Aster image showing regional tectonic structure, the 1985 Wuqia earthquake surface rupture and trench location. Modified from Li *et al.* (2012).



Fig. 2. Location of the modern sample LED11-7 (Left); Trench wall showing the location of samples LED11-1, 11-2 and 11-6 (Right).

The OSL samples were collected in stainless steel tubes (length 15–20 cm, diameter 6 cm). Both ends were immediately sealed with aluminium foil and taped to prevent light leakage and loss of water during transport and storage. The samples were extracted from the inner part of the tubes and quartz was purified using conventional sample preparation techniques (dissolving carbonates with 10% HCl, oxidizing organic matter with 10% H₂O₂, settling using Stokes' Law, dissolving feldspars by 30% fluorosilicic acid, followed by immersion in 10% HCl) for the 4–11 μm fine grain quartz (FQ) fraction (Aitken, 1998; Liu *et al.*, 2010), and 180–250 μm coarse grain quartz (CQ) fractions (sieving, 10% HCl, 10% H₂O₂, etching with 40% HF, followed by immersion in 10% HCl). The purity of the quartz extracts was confirmed by the absence of an IRSL signal for both FQ and CQ. Subsamples of FQ had IR signals close to background levels (Fig. 3a), with an IR-OSL depletion ratio between 0.9 and 1.1. Nevertheless, an IR-OSL depletion test (Duller, 2003) was carried out on every aliquot for small aliquot CQ and single grain (SG) quartz. All the D_e values of samples were measured on a Risø TL/OSL Reader model DA-20 equipped with a calibrated $^{90}\text{Sr}/^{90}\text{Y}$

beta radiation source (dose rate 0.1125 Gy/s for CQ and 0.1045 Gy/s for FQ in the standard configuration), blue ($470 \pm 30 \text{ nm}$; $\sim 50 \text{ mW/cm}^2$) and infrared ($880 \pm 40 \text{ nm}$, $\sim 145 \text{ mW/cm}^2$) light sources, and detection through a 7-mm thick U-340 glass filter.

Luminescence characteristics

We carried out dose recovery tests on sample LED11-6 (180–250 μm quartz). Eighteen aliquots were first bleached by sunlight in groups of three, then given a known laboratory beta dose (10 Gy), after which the standard SAR-protocol (Murray and Wintle, 2000) was applied using six different preheat and cutheat temperatures (preheat for 10 s at 180–280°C) followed by cutheat 40°C lower than preheat). The measured dose is indistinguishable from the known given dose at preheat temperatures of 260°C and cutheat 220°C (Fig. 3b). In addition, we applied a dose recovery test to 24 single quartz grain using a 260°C preheat for 10 s and a 220°C cutheat, with results showing that the average dose recovery ratio is 0.99 (Fig. 3d).

Based on the above results, a preheat of 260°C and a cutheat of 220°C were selected for all the samples.

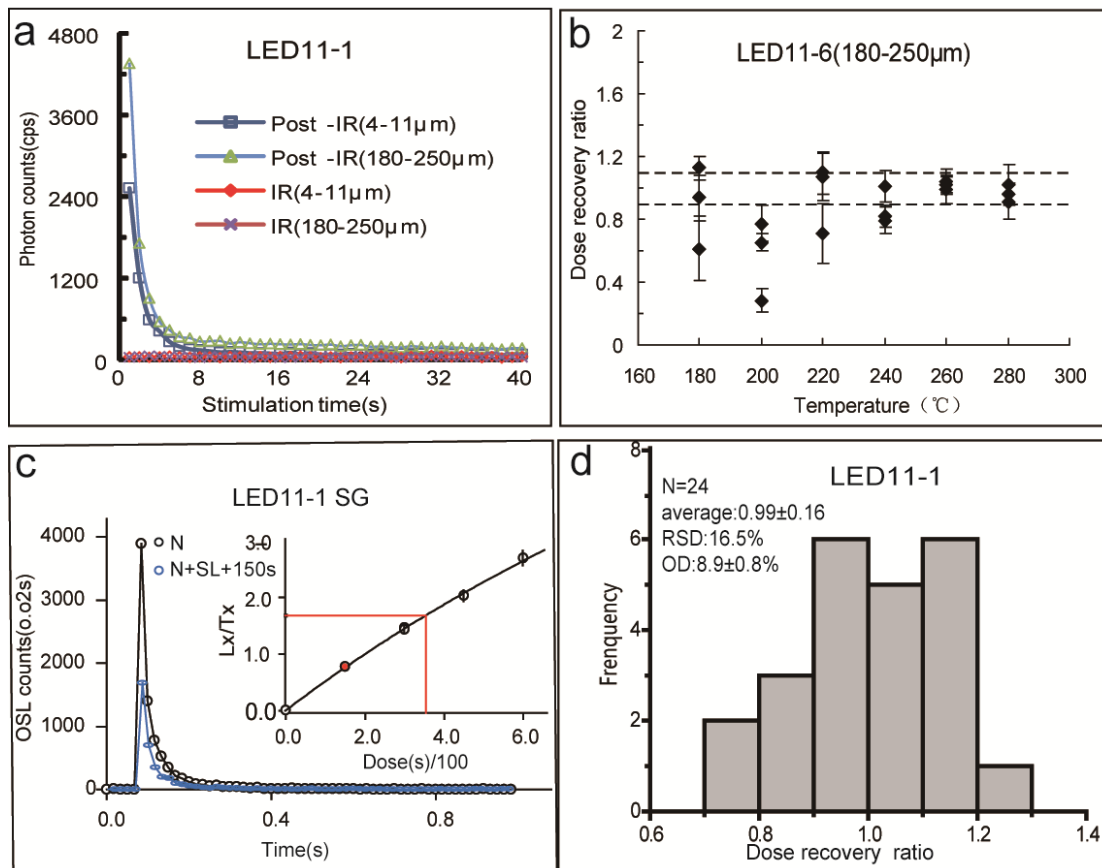


Fig. 3. Luminescence characteristics. a – Quartz purity IR check; b – Dose recovery as a function of preheat temperature for coarse grains quartz; c – OSL decay curves for single quartz grains from sample LED11-1, the inset shows a corresponding dose response curve (DRC), the red point is recycling point; d – A histogram of dose recovery ratios for single quartz grains using a 10 s preheat at 260°C for and a 220°C cutheat.

Equivalent dose measurements

Fine grain and single grain quartz

The FQ were measured using a sensitivity-corrected (by a test dose) multiple aliquot regenerative-dose (SMAR) protocol (Lu *et al.*, 2007; Liu *et al.*, 2010). At least six aliquots were measured to determine the natural OSL intensity, and the dose response curve (DRC) was constructed from five aliquots that brackets the natural (normalized) OSL signal (Fig. 4a). In general, the D_e values of the fine grain quartz using SMAR protocol are similar to those of the SAR protocol (Lu *et al.*, 2007; Liu *et al.*, 2010; Yang *et al.*, 2012). We have compared the results of SMAR and SAR protocol of the fine grain quartz for one sample. Both results are the same. But the SMAR protocol can save much more measurement time. So we used the SMAR protocol for fine grain size quartz.

We used the SAR protocol (Murray and Wintle, 2000, 2003; Kortekaas *et al.*, 2007) for the SG quartz measurements. Typical natural and regenerative luminescence signals are shown in Fig. 3c.

Small aliquot coarse grain quartz standardised growth curve (SA-SGC)

Single grain results show that only 1.5–3.7% of the grains yield a detectable OSL signal, a very time consuming endeavour considering that >95% of the grains were without any signal. To improve efficiency, we measured very small aliquots (~80–220 grains per disc as observed under the microscope), as most likely only one or two quartz grains on each disc give a signal, mimicking single grain measurements (Arnold *et al.*, 2012; Medialdea *et al.*, 2014; Faershtein *et al.*, 2016). The SA-SGC was used to measure a large number of D_e values: first a well constrained SAR DRC was constructed for each sample using 5–7 large aliquots from each sample (Fig. 4c), then the L_n/T_n , a zero dose point and one regenerative dose point were measured for a large number (up to 144) of small aliquots (Fig. 4d). The L_n/T_n of each individual small aliquot was projected on the sample-specific DRC to calculate the D_e for that particular aliquot. Aliquots were rejected if the single regenerative dose point did not lie on the SA-SGC within SA-SGC errors. This proce-

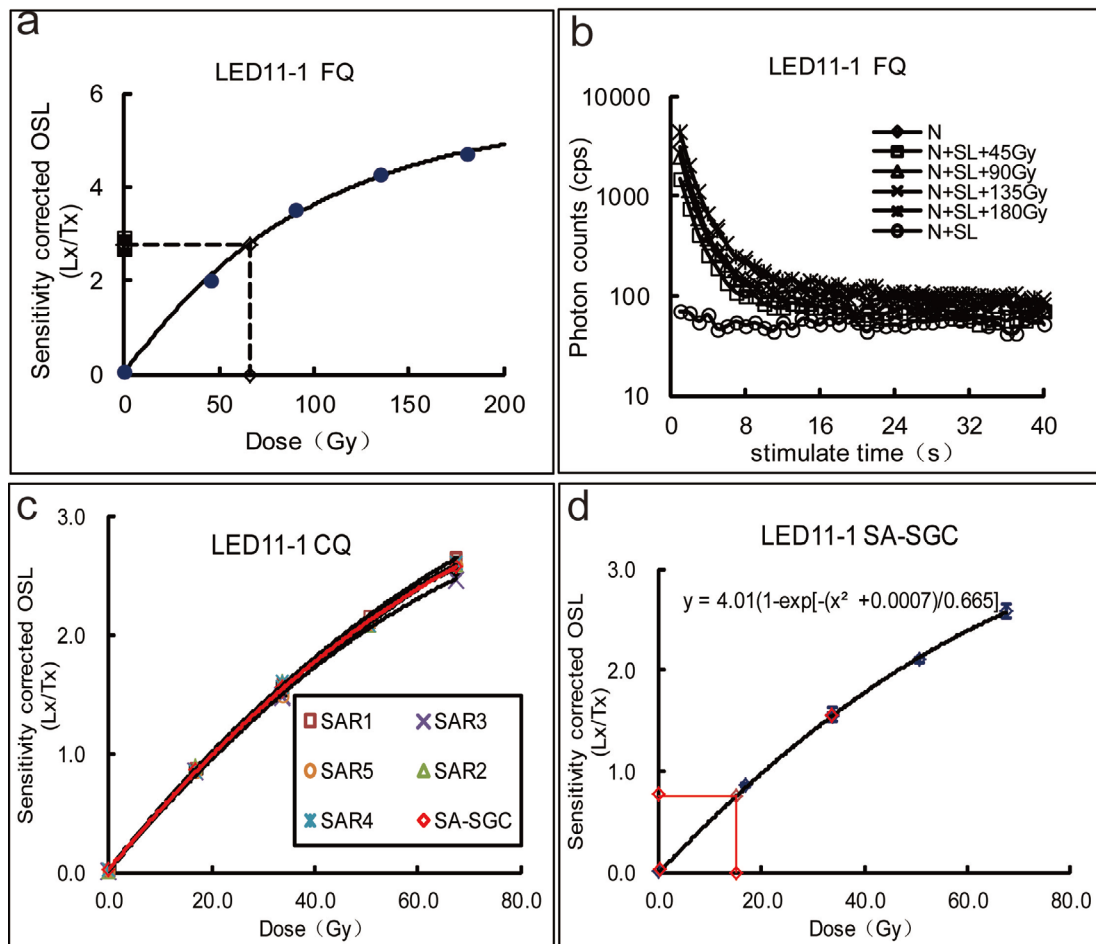


Fig. 4. a – Sensitivity-corrected multiple aliquot regenerative-dose growth curve (SMAR) of sample LED11-1; b – OSL decay curves of sample LED11-1; c – A SAR growth curve; d – Coarse grain quartz small aliquot standardized growth curve (SA-DRC). The red diamonds are sample-specific and were projected on the SA-DRC.

ture is advantageous for samples with heterogeneous resetting of the OSL signal prior to deposition, as it allowed rapid measurements of a large number of small aliquots that could be later used for calculating a meaningful D_e (Table 2).

Data analysis

For FQ, D_e values were calculated using the sum of photons detected in the first 1 s of the stimulation minus the average of the last 10 s (background) of the OSL decay curve.

OSL data from single grains and small aliquot were analyzed using the Risø Analyst software V4.31 and DRC was fitted by the exponential function for all the datasets. The D_e for small aliquots was calculated using early background subtraction (*i.e.*, the signal integrated from the first 0.32 s and background integrated from the next 0.96 s). The D_e for a single grain was calculated by integrating channels 4–10 (of 250 channels, 1 s stimulation) and subtracting the background from channels 40–50. Aliquots or grains were rejected if any of the following criteria applied: (1) no natural signal was present; (2) test dose error were >10%; (3) the response to the test-dose was less than 3 standard deviations above background; or (4) the recycling ratio or IR-OSL depletion ratio (Duller, 2003) were not consistent within 10% (15% for single grains) of unity. A 3.0% and 2.0% measurement error was incorporated for single grain data (Duller, 2006) and small aliquot data (estimated from Armitage *et al.*, 2000; Duller, 2007), respectively. We consider the

uncertainty sources for every aliquot or grain final D_e included counting statistics, curve fitting error, instrument reproducibility uncertainty of 1.5% (Risø Analyst Manual).

Dose rates

The U, Th, and K contents were measured by inductively coupled plasma mass spectrometer in Genalysis Laboratory Service, Australia, and the values are given in Table 1. Water content is from fresh sample we measured $5 \pm 5\%$ for the bottom sample LED11-1, 11-2 and $2 \pm 2\%$ for the above sample LED11-6, 11-7. A relative uncertainty of 100% was assigned to all moisture content measurements, to accommodate the effects of any potential variations during antiquity. The samples are above groundwater level and the current water content may have been constant over the whole burial span of the sediment. The dose rate for each sample is calculated directly by using the observed radionuclide concentrations and attenuation values from Aitken (1998). All the samples are above groundwater level and the water content was assumed to be $5 \pm 5\%$ for the bottom sample LED11-1, LED11-2 and $2 \pm 2\%$ for sample LED11-6 and LED11-7. α efficiency compared to beta irradiation of 0.04 ± 0.02 for fine-grained quartz was used, as suggested by Rees-Jones (1995) and Lu *et al.* (2007). Cosmic dose rates were evaluated using present day burial depths. The dose rates are given in Table 1 and are similar for all samples, ranging from 2.0 to 2.7 Gy/ka for coarse grain and 2.5 to 3.4 Gy/ka for fine grains (Table 1).

Table 1. Dose rate results for the samples.

Sample No.	Depth (m)	U (ppm)	Th (ppm)	K (%)	Water content ^a (%)	Dose rate (Gy/ka)	
						CQ	FQ
LED11-1	2.4	1.65	5.3	1.37	5 ± 5	2.1 ± 0.1	2.9 ± 0.2
LED11-2	2.8	1.74	4.84	1.15	5 ± 5	2.0 ± 0.1	2.6 ± 0.1
LED11-6	0.6	1.96	7.75	1.49	2 ± 2	2.7 ± 0.2	3.4 ± 0.2
LED11-7	0.2	1.35	4.67	1.2	2 ± 2	2.1 ± 0.1	2.5 ± 0.1

^a Water contents were estimated at $5 \pm 5\%$ or $2 \pm 2\%$

Table 2. D_e values of single grains, small aliquot SA-SGC and fine grains for the samples shown on Fig 2.

Sample No.	Single grains					Small aliquot SA-SGC					Fine grains	
	n/N ^a	P ^b (%)	OD ^c (%)	D_e^d (Gy)	Age (ka)	n/N ^a	P ^b (%)	OD ^c (%)	D_e^d (Gy)	Age (ka)	D_e (Gy)	Age (ka)
LED11-1	158/4800	3.3	45	$14.3^{+1.9}_{-1.7}$	$6.7^{+1.0}_{-0.9}$	43/78	55	36	$14.3^{+3.3}_{-3.0}$	$6.7^{+1.6}_{-1.5}$	65.7 ± 5.4	22.9 ± 1.9
LED11-2	55/2300	2.4	62	$9.6^{+2.5}_{-1.9}$	$4.9^{+1.3}_{-1.0}$	63/142	44	59	$9.8^{+3.0}_{-1.8}$	$5.0^{+1.6}_{-1.0}$	157.6 ± 14.3	60.5 ± 5.4
LED11-6	55/3700	1.5	45	$5.2^{+1.4}_{-1.0}$	$2.0^{+0.5}_{-0.4}$	52/144	40	33	$5.4^{+1.5}_{-0.5}$	$2.0^{+0.6}_{-0.2}$	66.8 ± 3.1	19.5 ± 0.9
LED11-7	53/1800	2.9	80	$0.2^{+0.2}_{-0.1}$	$0.1^{+0.1}_{-0.05}$	42/88	47	59	$0.3^{+0.3}_{-0.2}$	$0.15^{+0.15}_{-0.1}$	7.0 ± 0.3	2.8 ± 0.1

^a n represents the number of accepted single grains or small aliquots that passed the SAR rejection criteria and used for D_e determination, N represents total number of grains or aliquots measured;

^b Proportion (%) of the grains or aliquots that have a detectable OSL signal;

^c over-dispersion;

^d D_e obtained using the minimum age model.

3. RESULTS

As **Table 2** shows, the D_e values of FQ range from 7.0 Gy to 158 Gy and the ages from 2.8 ka to 60.5 ka. For SG, we measured a sufficient number of grains so that there were more than fifty accepted for every sample. The percentage of grains with detected signal is lower than 4%. The over-dispersion values range from 45% to 80%. They are higher than average value 20% comparing with the global overdispersion datasets (Arnold and Roberts, 2009). It may be caused different by degrees of the signal resetting. Therefore we used the four parameter version of the minimum age model (Galbraith *et al.*, 1999) which can be used by a likelihood ratio test such as the maximum log likelihood (L_{max} higher than 1.92) to isolate the best bleached grains and calculate the most representative D_e values. In the four-parameter version (MAM-4), δ_i is drawn from a population in which a proportion ρ of values are equal to τ and the remaining values are larger, having a normal distribution with parameters μ and σ truncated at τ . Therefore, $\exp(\tau)$ represents the minimum true dose (in Gy) of the population (Arnold *et al.*, 2009). Prior to running the MAM-4, we added, in quadrature, an overdispersion value of 20% to each individual measured D_e error, to represent the underlying dose overdispersion typically present in well-bleached and undisturbed samples (Arnold and Roberts, 2009; Arnold *et al.*, 2009). The D_e values and ages range from $0.2^{+0.2}_{-0.1}$ Gy to $14.3^{+1.9}_{-1.7}$ Gy and from $0.1^{+0.1}_{-0.05}$ ka to $6.7^{+1.0}_{-0.9}$ ka, respectively. For the same samples we measured at least forty accepted small aliquots that passed the SAR rejection criteria for each sample using CQ SA-SGC. The proportion of the accepted aliquots, 40–55%, is much higher than for single grains, and the over-dispersion values range from 33% to 59%, lower than for SG. The D_e values and ages range from $0.3^{+0.3}_{-0.2}$ Gy to $14.3^{+3.3}_{-3.0}$ Gy and from $0.15^{+0.15}_{-0.1}$ ka to $6.7^{+1.6}_{-1.5}$ ka, respectively.

4. DISCUSSION

Our study compared OSL ages from different grain-size fractions with different techniques based on the same sample. Ideally a sample should give similar ages for different grain-size fractions and different protocols, but this was not the case. We have one modern sample (LED11-7) deposited after 1985 as an independent age control. We did not find any carbon in the sequence. The depositional environments are fluvial and pluvial deposition in the arid mountainous regions. For FQ, the ages in the trench section are not in chronological sequence and all the ages are much older than the cosmogenic ^{10}Be ages of 8–8.8 ka. The age of the modern sample LED11-7 is 2.8 ± 0.1 ka, overestimating the true modern age. D_e values of the FQ are 5 to 17 times higher than CQ. The apparent overestimation of OSL ages most likely results from the different aliquot size used for fine and coarse

grains. For each of these different measurements, there is a very different number of grains on the disc that contribute to the luminescence signal. Roughly one million grains are present on a fine grain aliquot, an abundance that averages any grain-to-grain dose variations (Wallinga, 2002; Duller, 2008). This averaging masks the poorly bleached grains and results in an overestimation of the true depositional age of the sediment. Therefore fine grain quartz OSL dating is not suitable for such pluvial sediment in association with paleo-earthquakes.

SG ages show a good chronological sequence in the trench section. The MAM age of the modern sample LED11-7 is $0.1^{+0.1}_{-0.05}$ ka, sufficiently close to the zero. It shows that this modern analogue is representative of depositional environments, partial bleaching is not the cause using single grains and coarse grain SA-SGC. The lowest sample from the trench located on the terrace (LED11-1) gave a MAM age of $6.7^{+1.0}_{-0.9}$ ka, consistent with the cosmogenic ^{10}Be . Using single grains can separate the best bleached grains from the entire grain population, implying that the single grain results are much closer to the true ages. We suggest that SG measurements combined with the appropriate model is suitable for optical dating of poorly bleached sediments associated with paleo-earthquakes, a conclusion similar to that reached by Porat *et al.* (2009).

The small aliquots of the SA-SGC have ~80–220 grains per disc; with the small fraction of luminescent grains (1.5–3.7% of the grains emit a luminescence signal according to the single grain results), only 1–2 grains give a luminescence signal on each small aliquot. In addition, the D_e values and ages obtained by the SA-SGC are, within errors, the same as those measured for single grains. In fact, the D_e value calculated for sample LED11-2 using 49 (2-mm) aliquots is $19.5^{+6.4}_{-3.8}$ Gy, however when additional smaller aliquots were measured (~50–120 grains, 1 mm disc), a D_e of $9.8^{+3.0}_{-1.8}$ Gy was obtained using MAM3, similar to the single grains results. Measuring coarse grain quartz using SA-SGC instead of SG provides a time-saving procedure when dating heterogeneously bleached sediments, with results similar to that of SG. But it is necessary to ensure that there is a small enough number of grains on a disc and enough accepted aliquots.

5. CONCLUSIONS

In this study, fine grains quartz measurements overestimated the expected D_e values and were much older than single grains and coarse grain SA-SGC. The residual dose of $0.2^{+0.2}_{-0.1}$ Gy measured using single grains of the modern sample is insignificant when dating samples which are thousands of years old in paleo-earthquake settings. Only 1.5–3.6% of the coarse-grain quartz have a detectable OSL signal. The ages measured for three samples in the trench section using single grains are in stratigraphic

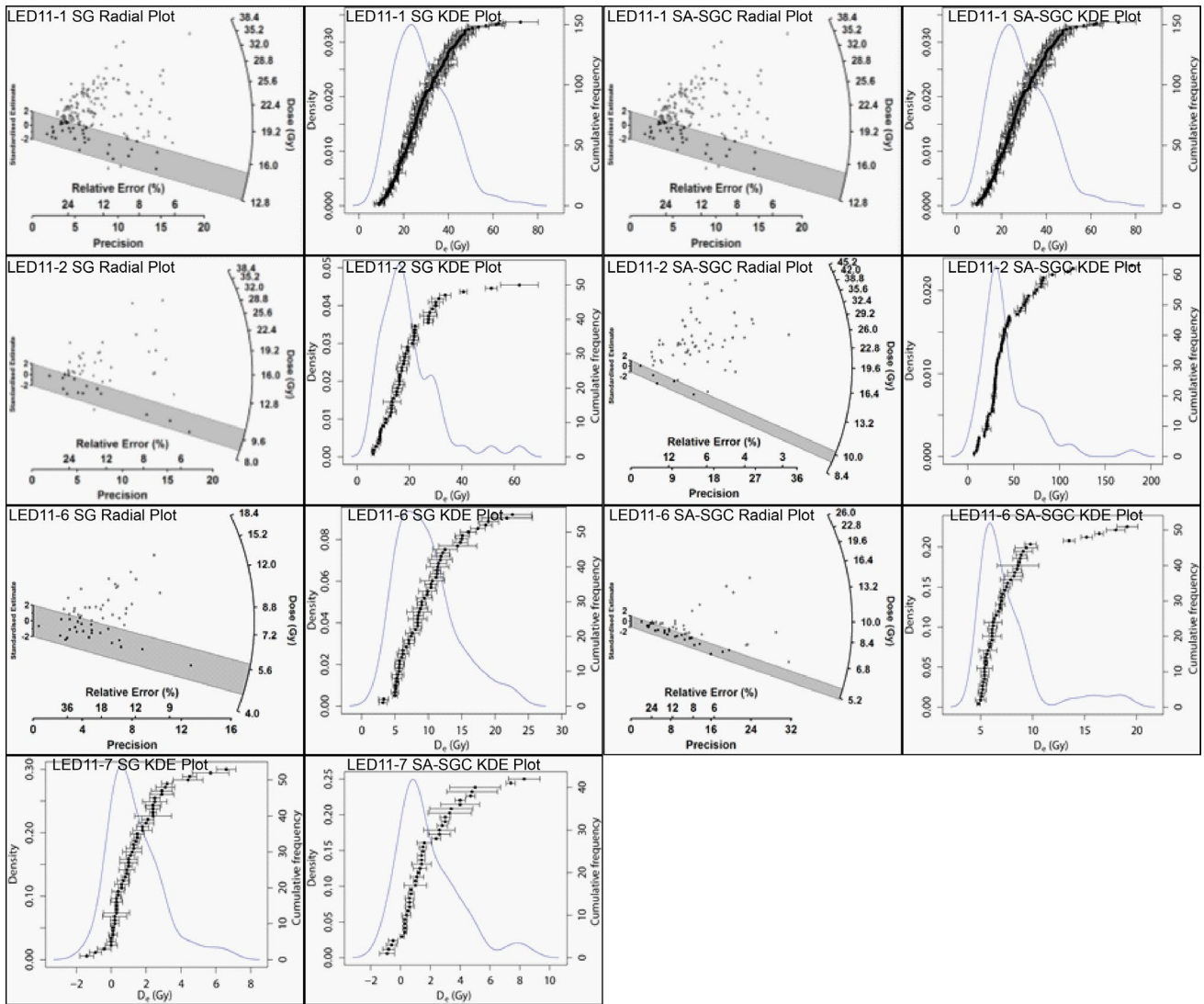


Fig. 5. Radial plots and KDE plots from single grains (SG) and small aliquot standardised growth curve (SA-SGC) for samples LED11-1, LED11-2 and LED11-6. Grey bands on radial plots show the samples' D_e values with 2-sigma error (Table 2). Only KDE plots are shown for the sample LED11-7.

sequence and are consistent with that of the cosmogenic ^{10}Be dating, indicating that such samples might be suitable for optical dating of paleo-earthquakes. Coarse grains SA-SGC D_e values are similar to those measured for single grains. This is an efficient way to measure poorly bleached quartz which has good potential for future studies of paleo-earthquakes. Notably, enough accepted grains or aliquots are required for calculating D_e values. Detailed and thorough scientific studies should be carried out in order to improve accuracy for paleo-earthquake ages. We recommend using caution when interpreting ages derived from fine grain measurements.

ACKNOWLEDGMENTS

This work was supported by the National Natural Science Foundation of China (41702222) and Basic Scientific Research Fund, Institute of Geology, China Earthquake Administration (IGCEA1418) and State Key Lab. of Earthquake Dynamics of China (LED2016A05) and the International Science and Technology Cooperation Program of China (2008DFA20860). This manuscript was significantly improved by thoughtful comments and suggestions from two anonymous reviewers and the associate editor L.J. Arnold.

REFERENCES

- Aitken MJ, 1998. *An Introduction to Optical Dating: The Dating of Quaternary Sediments by the Use of Photon-stimulated Luminescence*. Oxford University Press, Oxford.
- Armitage SJ, Duller GAT and Wintle AG, 2000. Quartz from southern Africa: sensitivity changes as a result of thermal pretreatment. *Radiation Measurements* 32(5–6): 571–577, DOI 10.1016/S1350-4487(00)00053-6.
- Arnold LJ and Roberts RG, 2009. Stochastic modelling of multi-grain equivalent dose (D_e) distributions: implications for OSL dating of sediment mixtures. *Quaternary Geochronology* 4: 204–230, DOI 10.1016/j.quageo.2008.12.001.
- Arnold LJ, Roberts RG, Galbraith RF and DeLong SB, 2009. A revised burial dose estimation procedure for optical dating of young and modern-age sediments. *Quaternary Geochronology* 4: 306–325, DOI 10.1016/j.quageo.2009.02.017.
- Arnold LJ, Demuro M and Navazo Ruiz M, 2012. Empirical insights into multi-grain averaging effects from ‘pseudo’ single-grain OSL measurements. *Radiation Measurements* 47: 652–658, DOI 10.1016/j.radmeas.2012.02.005.
- Banerjee D, Murray AS and Foster IDL, 2001. Scilly Isles, UK: optical dating of a possible tsunami deposit from the 1755 Lisbon earthquake. *Quaternary Science Reviews* 20: 715–718, DOI 10.1016/S0277-3791(00)00042-1.
- Cunha PP, Buylaert JP, Murray AS, Andrade C, Freitas MC, Fatela F, Munhá JM, Martins AA and Sugisaki S, 2009. Optical dating of clastic deposits generated by an extreme marine coastal flood: the 1755 tsunami deposits in the Algarve (Portugal). *Quaternary Geochronology* 5(2–3): 329–335, DOI 10.1016/j.quageo.2009.09.004.
- Duller GAT, 2003. Distinguishing quartz and feldspar in single grain luminescence measurements. *Radiation Measurements* 37: 161–165, DOI 10.1016/S1350-4487(02)00170-1.
- Duller GAT, 2006. Single grain optical dating of glaciogenic deposits. *Quaternary Geochronology* 1(4): 296–304, DOI 10.1016/j.quageo.2006.05.018.
- Duller GAT, 2007. Assessing the error on equivalent dose estimates derived from single aliquot regenerative dose measurements. *Ancient TL* 25: 15–24.
- Duller GAT, 2008. Single-grain optical dating of Quaternary sediments: why aliquot size matters in luminescence dating. *Boreas* 37: 589–612, DOI 10.1111/j.1502-3885.2008.00051.x.
- Fattahi M, Nazari H, Bateman MD, Meyer B, Sébrier M, Talebian M, Le Dortz K, Foroutan M and Ahmad Givi Fand Ghorashi M, 2010. Refining the OSL age of the last earthquake on the Dshshir fault, Central Iran. *Quaternary Geochronology* 5(2–3): 286–292, DOI 10.1016/j.quageo.2009.04.005.
- Feng XY, Yang Z and Luan CQ, 1986. The WuQia earthquake of Xinjiang. *Earthquake Research In China* 2(1): 56–60.
- Fuchs M, Straub J and Zoller L, 2005. Residual luminescence signals of recent river flood deposits: A comparison between quartz and feldspar of fine- and coarse-grain sediments. *Ancient TL* 23: 25–30.
- Faershtein G, Porat N, Avni Y and Matmon A, 2016. Aggradation–incision transition in arid environments at the end of the Pleistocene: An example from the Negev Highlands, southern Israel. *Geomorphology* 253: 289–304, DOI 10.1016/j.geomorph.2015.10.017.
- Lai ZP, Bruckner H, Zoller L and Fulling A, 2007. Existence of a common growth curve for silt-sized quartz OSL of loess from different continents. *Radiation Measurements* 42: 1432–1440, DOI 10.1016/j.radmeas.2007.08.006.
- Kortekaas M, Murray AS, Sandgren P and Björck S, 2007. OSL chronology for a sediment core from the southern Baltic Sea: a continuous sedimentation record since deglaciation. *Quaternary Geochronology* 2(1–4): 95–101, DOI 10.1016/j.quageo.2006.05.036.
- Li B, Roberts RG, Jacobs Z and Li SH, 2015. Potential of establishing a ‘global standardized growth curve’ (gSGC) for optical dating of quartz from sediments. *Quaternary Geochronology* 27: 94–104, DOI 10.1016/j.quageo.2015.02.011.
- Li T, Chen J, Thompson JA, Burbank DW and Xiao W, 2012. Equivalency of geologic and geodetic rates in contractional orogens: New insights from the Pamir Frontal Thrust. *Geophysical Research Letters* 39: L15305, DOI 10.1029/2012GL051782.
- Liu JF, Chen J, Yin JH, Lu YC, Murray AS, Chen LC, Thompson J, Yang HL, 2010. OSL and AMS ^{14}C dating of the Penultimate earthquake at the Leigu trench along the Beichuan Fault, Longmen Shan, in the Northeast margin of the Tibetan plateau. *Bulletin of the Seismological Society of America* 100: 2681–2688, DOI 10.1785/0120090297.
- Lu YC, Wang XL and Wintle AG, 2007. A new OSL chronology for dust accumulation in the last 130,000 yr for the Chinese Loess Plateau. *Quaternary Research* 67(1): 152–160, DOI 10.1016/j.yqres.2006.08.003.
- Medialdea A, Thomsen KJ, Murray AS and Benito G, 2014. Reliability of equivalent-dose determination and age-models in the OSL dating of historical and modern palaeoflood sediments. *Quaternary Geochronology* 22: 11–24, DOI 10.1016/j.quageo.2014.01.004.
- Murray AS and Wintle AG, 2000. Luminescence dating of quartz using an improved single-aliquot regenerative-dose protocol. *Radiation Measurements* 32: 57–73, DOI 10.1016/S1350-4487(99)00253-X.
- Murray AS and Wintle AG, 2003. The single aliquot regenerative dose protocol: potential for improvements in reliability. *Radiation Measurements* 37: 377–381, DOI 10.1016/S1350-4487(03)00053-2.
- Olley JM, Caitcheon G and Murray A, 1998. The distribution of apparent dose as determined by optically stimulated luminescence in small aliquots of fluvial quartz: implications for dating young sediments. *Quaternary Geochronology* 17:1033–1040, DOI 10.1016/S0277-3791(97)00090-5.
- Porat N, Duller GAT, Amit R, Zilberman E and Enzel Y, 2009. Recent faulting in the southern Arava, Dead Sea Transform: Evidence from single grain luminescence dating. *Quaternary International* 199: 34–44, DOI 10.1016/j.quaint.2007.08.039.
- Rees-Jones J, 1995. Optical dating of young sediments using fine-grain quartz. *Ancient TL* 13(2): 9–14.
- Roberts HM and Duller GAT, 2004. Standardised growth curves for optical dating of sediment using multiple-grain aliquots. *Radiation Measurements* 38: 241–252, DOI 10.1016/j.radmeas.2003.10.001.
- Thompson JA, 2013. *Neogene tectonic evolution of the NE Pamir margin, NW China*. UC Santa Barbara. PhD thesis.
- Wang XL, Chai ZZ, Du P, Lei QY, Yin GM and Lu YC, 2012. Luminescence age constraints on palaeo-earthquake events along the LingWu fault in the YinChuan basin, China. *Geochronometria* 39(1): 57–61, DOI 10.2478/s13386-011-0051-4.
- Wallinga J, 2002. Optically stimulated luminescence dating in fluvial deposits: A review. *Boreas* 31: 303–322, DOI 10.1111/j.1502-3885.2002.tb01076.x.
- Yang HL, Chen J, Jessica AT and Liu JF, 2012. Optical dating of the 12 May 2008, Ms 8.0 Wenchuan earthquake-related sediments: Tests of zeroing assumptions. *Quaternary Geochronology* 10: 273–279, DOI 10.1016/j.quageo.2012.02.022.